In silico modeling and empirical study of 4-nButylresorcinol nanoliposome formulation

by Rini Dwiastuti

Submission date: 14-Apr-2023 09:37PM (UTC+0700)
Submission ID: 2064447835
File name: JBSD_Juli_2021.pdf (2.58M)
Word count: 7674
Character count: 41894

12
Journal of Biomolecular Structure and Dynamics

ISSN: (Print) (Online) Journal homepage: https://www.tandfonline.com/loi/tbsd20

In silico modeling and empirical study of 4-*n*-Butylresorcinol nanoliposome formulation

11
Rini Dwiastuti, Muhammad Radifar, Dina Christin Ayuning Putri, Florentinus Dika Octa Riswanto & Maywan Hariono

6
To cite this article: Rini Dwiastuti, Muhammad Radifar, Dina Christin Ayuning Putri, Florentinus Dika Octa Riswanto & Maywan Hariono (2021): *In silico* modeling and empirical study of 4-*n*-Butylresorcinol nanoliposome formulation, Journal of Biomolecular Structure and Dynamics, DOI: 10.1080/07391102.2021.1946430

To link to this article: https://doi.org/10.1080/07391102.2021.1946430

Published online: 08 Jul 2021.

JOURNAL OF BIOMOLECULAR STRUCTURE AND DYNAMICS
https://doi.org/10.1080/07391102.2021.1946430

Taylor & Francis
Taylor & Francis Group

In silico modeling and empirical study of 4-*n*-Butylresorcinol nanoliposome formulation

Rini Dwiastuti[a], Muhammad Radifar[b], Dina Christin Ayuning Putri[a], Florentinus Dika Octa Riswanto[c] and Maywan Hariono[c]

[a]Department of Pharmaceutical Technology, Faculty of Pharmacy, Sanata Dharma University, Yogyakarta, Indonesia; [b]Medical Laboratory Technology, Guna Bangsa Institute of Health Science, Yogyakarta, Indonesia; [c]Department of Pharmaceutical Analysis and Medicinal Chemistry, Faculty of Pharmacy, Sanata Dharma University, Yogyakarta, Indonesia

Communicated by Ramaswamy H. Sarma

ABSTRACT

A study to incorporate *in silico* modeling with an empirical experiment has been carried out to formulate nanoliposome containing 4-*n*-butylresorcinol as the active ingredient. The *in silico* modeling was performed using molecular dynamics simulation followed by radius of gyration observation to provide insight into the mechanisms of 4-*n*-butylresorcinol stabilization by liposome due to their nano-size. The empirical experiment was conducted by formulating the nanoliposome using soy lecithin phospholipid formula as suggested by the *in silico* modeling followed by determining its particle size as well as its shape. From their incorporation, it was found that 3200 phospholipid molecules were selected in formulating nanoliposome containing 4-*n*-butylresorcinol. The results of the nanoliposomes size observation in the modeling of 3200 lipid molecules was 87.01 (± 0.59) nm, whereas the size from the empirical study was 87.57 (± 0.06) nm.

List of abbreviation: LUV: Large Unilamellar Vesicles; SUV: Small Unilamellar Vesicles; AFA: Adaptive Focused Acoustics™; CGMD: Coarse-Grained Molecular Dynamic; DMPC: dimyristoyl-phosphatidylcholine; DPPC: dipalmitoyl-phosphatidylcholine; TEM: Transmission Electron Microscopy; PIPC: palmitoyllinoleyl-phosphatidylcholine; vdW: van der Waals

ARTICLE HISTORY
Received 5 February 2021
Accepted 17 June 2021

KEYWORDS
nanoliposome; 4-n-butylresorcinol; formulation; in silico modeling; simulation

Introduction

Nanoparticle technology has become one of the trending interests in drug delivery system research in the last decade (Boisseau & Loubaton, 2011; Puri et al., 2009). Applied technology in nanoparticle formulation can be performed using two different methods, namely top-down and bottom-up methods (Singh et al., 2011; Reverchon & Adami, 2006). Drug delivery system improvement using lipid nanoparticle formulation has been developed by arranging phospholipid bilayer fragments as well as liposomes for a diverse administration route in the human body. Lipid nanoparticle formulation provides several advantages such as low toxicity, which is proven by *in vivo* observation and its capability to improve the physical stability of the active ingredient in the dosage form formulation (Akbarzadeh et al., 2013). Nanoparticle technology can be applied in the drug formulation with the encapsulation process by several matrices such as nanospheres, nanoliposomes, and nanoemulsions (Martien et al., 2012).

One of the lipid nanoparticle drug delivery systems that has been commonly developed is nanoliposome since it has been reported to have several advantages such as increasing the efficacy and therapeutic index as well as improving the drug stability through the encapsulation system (Akbarzadeh et al., 2013). Liposome, a topical dosage form, has been developed in the drug formulation due to its good penetration into the skin (El Maghraby et al., 2010; El Maghraby et al., 2010). Nanoliposome showed good activity of penetrating the cell wall and intercellular space due to their nano-size, i.e. $<$ 200 nm (Reverchon & Adami, 2006). The trend of nanoliposome formulation development increased continuously since the formulation process was reported to play an essential role in drug encapsulation (Wang et al., 2011; Zhao et al., 2009). The physical stability of the dosage form could be maintained by increasing the drug encapsulation and reducing the liposome leakage during the storage (Eloy et al., 2014; Laouini et al., 2012).

Nevertheless, several formulation problems were found during the formulation of nanoliposomes such as the time-consuming process, organic solvent selection consideration, and economical consideration for performing trial and error formulation. Computational methods have been used to predict drug delivery systems before drug formulations. It aims to minimize investment in drug design and development (Li & Hou, 2010). The modeling of liposome formation molecules with phospholipids 1,2- dipalmitoyl-sn-glycero-3-phosphatidylcholine had been carried out by Koshiyama and Wada (2016), showing that the formed liposomes have different

CONTACT Rini Dwiastuti rini_dwi@usd.ac.id Department of Pharmaceutical Technology, Faculty of Pharmacy, Sanata Dharma University, Yogyakarta 55282, Indonesia

shapes and sizes depending on the number of phospholipids being used. A study related to *in silico* modeling of liposome formation had also been carried out by Dwiastuti et al. (2018) using 1,2-dilauroyl-sn-glycero-3- phosphatidylethanolamine producing almost the same shape and size of the liposomes in empirical experiments. The difference between the two studies is the software being used in the *in silico* modeling simulation. However, it has not been supported by empirical verification of the liposome manufacture. All of these problems can be overcome by generating an accurate prediction, taking into account the atomic interaction between the drug and its delivery system using appropriate molecular modeling simulation (Hashemzadeh et al., 2020). Furthermore, the number of water and lipid molecules obtained from the *in silico* modeling is correlated with the empirical observations of the liposome formation. The conversion factor should be calculated to obtain a quantitative correlation of phospholipid numbers used both for simulation modeling and empirical observation (Jämbeck et al.,2014). The *in silico* modeling of liposome formation can be applied in a formulation study by employing mathematical prediction to achieve a good nanoliposomes drug delivery system supported by the computational approach (Dogra et al., 2019; Cern et al., 2017; Cern et al., 2014).

One of the liposome formulation methods is a lipid dispersion in an aqueous media with sonication along with controlling its temperature, which is the easiest method (Akbarzadeh et al., 2013). The previous study by Shen et al. (2015) had empirically approached the formulation of Large Unilamellar Vesicles (LUV) or Small Unilamellar Vesicles (SUV) liposomes using focused ultrasonic irradiation with the usage of Adaptive Focused Acoustics™ (AFA) (Shen et al., 2015). This applied method was performed at a low temperature without organic solvent and produced liposomes with a size of < 600 nm. One way to reduce trial and error in experimental study is by using *in silico* modeling to predict the formation of liposomes sub-molecularly (Trisilowati and Mallet, 2012). The lipid dispersion in aqueous media with sonication energy and its controlled temperature can be used as the system in the modeling approach, which is the first step before starting the empirical study. Furthermore, the *in silico* modeling study should be compared with the empirical observations to obtain a correlation between the number of phospholipid molecules resulted from the modeling with the number of phospholipid molecules in the empirical study.

In silico modeling in this study was described as a computational approach to study the interaction between drug molecules with the liposome phospholipid membrane and to present the whole molecular interaction during the liposome formation. Risselada and Marrink (2009) studied the effect of temperature and membrane composition during the simulation process towards the structure and dynamic behavior of the liposome membrane with the diameter of 15-20 nm using Coarse-Grained Molecular Dynamic (CGMD) simulation (Risselada & Marrink, 2009). Another study by Siwko et al. (Siwko et al., 2009) was conducted on *in silico* modeling of dimyristoyl-phosphatidylcholine (DMPC) phospholipid which used CGMD at 323 K to investigate the interaction between resorcinol and the bilayer lipid membrane. The results showed that the presence of resorcinol interestingly increased the membrane stability of the lipid bilayer systems. Hudiyanti et al. (Hudiyanti et al., 2014) also employed the CGMD for simulating the *in silico* modeling to prepare liposomes from various phospholipids. In this study, three types of liposome (origin, deformed liposome, and planar bilayer) were *in silico* simulated to interact with water, to give an insight understanding on which type of liposome will give the most stable structure during 160 ns of the simulation time. Therefore, the use of CGMD in drug delivery system modeling has been commonly used to provide the best formula in the liposome production.

In this present study, 4-*n*-butylresorcinol was used as the drug instead of resorcinol as the drug model. It functions as tyrosinase inhibitor for the management of pigmentation disorders, such as the topical treatment of hyperpigmentation (Kolbe et al., 2013). This resorcinol derivative is more stable than resorcinol due to the oxidation process (Love et al., 2005). A double-blind study for melasma with 4-*n*-butylresorcinol being applied twice daily within 8 weeks was necessary to achieve the hypopigmenting effect. However, 12 adverse events including mild erythema, dryness, peeling, and desquamation have appeared (Khemis et al., 2007). The 4-*n*-butylresorcinol was encapsulated in liposomes to improve the stability and to reduce skin irritation through hydration of the epidermis (Huh et al., 2010; De Leeuw et al., 2009). The stability should be improved by encapsulating the compound into the complex of nanoliposome structure. Encapsulating phenol-related compounds such as 4-*n*-butylresorcinol aims to preserve the biological activity and to improve the stability of the active compounds, as well as to ensure controlled release of the latter. Encapsulation has the advantage of being a non-thermal stabilization approach and is suitable for temperature-sensitive natural biologically active compounds. The wall material usually improves the stability of the active compounds by protecting them from direct exposure to air and light (Coradini et al., 2014; Love et al., 2005). The *in silico* modeling simulation in the initial step of the formulation was important to predict the physical properties of the lipid nanoparticle complex production. The formulation technique was necessarily developed to produce nanoliposomes with nano size ($<$100 nm) in a short time usage of sonication. It was reported that the heating and sonication processes were important in the nanoliposomes formulation. Mozafari et al. reported that the production of nanoliposomes with the size of $\pm$600 nm was successfully carried out by the heating process without any extrusion process in polycarbonate membrane as well as sonication (Mozafari et al., 2007). Another study reported that the particle size reduction ($\leq$ 100 nm) occurred with an increase of sonication time for more than 21 min (Silva et al., 2010). Hence, it is important to consider the correlation between the *in silico* modeling approach and empirical observational results in an integrated research. This study aims to correlate Molecular Dynamic (MD) simulation and an empirical observation in the production of nanoliposomes using soy lecithin phospholipid and 4-*n*-butylresorcinol as the delivery system and active ingredient, respectively.

Table 1. The nanoliposome formula on the empirical observation.

Materials	Amount
Soy lecithin	7.74 g
4-*n*-butylresorcinol	0.1% w/v
Re-distilled water	100.00 mL

Materials and methods

Materials

Soy lecithin phospholipid (Pharmaceutical Grade, Nacalai Tesque, Japan), redistilled water, 4-*n*-butylresorcinol (Pharmaceutical Grade, SHREEJI Pharma International, India), ethanol (Analytical Grade, Merck, USA).

Gas chromatography-mass spectrometry analysis (GC-MS) of soy lecithin

The GC-MS analysis was performed using a Shimadzu GCMS-QP2010S with Agilent HP-5ms column (30 m x 0.25 mm x 0.25 µm). The injector temperature was set to 310 °C. Helium was used as carrier gas at a constant flow rate of 0.40 mL/min. The column temperature was kept at 120 °C for 5 min and then increased from 120° to 300 °C at 5° C/min. As for the ion source, the temperature was set to 250° C, and the interface temperature was set to 305° C. The mass scanning was set from m/z 28 to 600.

Molecular dynamics simulation of soy lecithin

Coarse-grained Molecular Dynamics using MARTINI 2.0 force field was used to study the liposome formation of soy lecithin. Prior to the initial coordinate preparation, the coarse-grained structure of phospholipids (DPPC, POPC, and PIPC), cholesterol, and 4-*n*-butylresorcinol were prepared. The GC-MS analytical results were used to determine the composition of soy lecithin and to construct the initial coordinates according to the composition. The initial coordinate was prepared by a random placement of phospholipid and cholesterol in a $22 \times 22 \times 22\,nm^3$ box using the gmx insert-molecule module of GROMACS 2019.1 package on Centos 7.4. Three concentrations of lipids were used i.e. 2400, 2800, and 3200 lipids/boxes. Each concentration of lipid had two treatments, i.e. by adding 4-*n*-butylresorcinol and without 4-*n*-butylresorcinol (negative controls). The molecule numbers of 4-*n*-butylresorcinol being added were 123, 143, and 164 molecules for 2400, 2800, and 3200 lipids, respectively. In total, there are six different initial coordinates in a duplicate experiment. After the lipid was randomly placed, the box configuration was edited using a gmx edit conf module and solvated with 78,299 water beads using a gmx solvate module generating a system consisted of lipids and water with the size of $24 \times 24 \times 24\,nm^3$. The initial coordinates were then subjected to energy minimization using the gmx mdrun module with the steepest descent method. The resulting minimized system was then simulated under NPT condition for 240 ns using 40 fs time step, 323 K temperature, and reaction-field long-range electrostatic treatment. The temperature was controlled using the V-rescale method while the pressure was controlled using the Berendsen barostat. The MD results were then processed with gmx energy module to generate the potential energy data and gmx gyrate module to generate the radius of gyration data. The data were then plotted using Grace. The trajectory file was visualized using VMD 1.9.3 to understand the dynamic of the liposome assembly and the morphology of the liposome.

Empirical observations

The formulation of nanoliposomes with and without 4-*n*-butylresorcinol was carried out by dispersing an amount of soy lecithin over re-distilled water using the heating method and combined with sonication. The formula was composed of soy lecithin and other ingredients, as presented in Table 1. The empirical observation was approached by formulating the nanoliposomes using the theoretical data of soy lecithin through *in silico* modeling of 3200 phospholipid molecules. The phospholipid being used in this study was soy lecithin having the temperature transition between 50-60 °C (De Leeuw et al., 2009). The temperature in the formulation was set at 50 °C along with 30 min sonication and 37 kHz of a bath sonicator. Soy lecithin was dispersed in 100 ml of re-distilled water at 50 °C until the nanoparticle system met the requirement of a polydispersity index (< 0.3). The 50° C temperature used during the formulation was conducted to set the temperature condition close to the *in silico* modeling parameters. The soy lecithin dispersed solution was then blended at a high speed. This aimed to minimize the bilayer fragment sheets that had been formed. The solution was then homogenized using Ultraturac® for 1 min at four scales and sonicated for 30 min (Dwiastuti et al., 2016; Dwiastuti et al., 2018) until the particle with <100 nm in size were observed. The product was then left to cool down at room temperature before morphological and particle size testing were conducted. After that, the product was stored in a refrigerator at 4-8 °C.

The conversion of soy lecithin from molecular modeling into empirical observation

The soy lecithin used in the empirical observation was based on the number of phospholipid molecules in nanoliposomes modeling. The concentration of phospholipid in the simulation of 3200 phospholipid molecules was 387.12 mg/mL, which equals to 0.38712 g/mL.

$$\text{The amount of soy lecithin used} : \frac{0.38712\ g/mL\ x(\text{thebox size in modeling})}{100nm}$$
$$: 0.38712\ g/mL\ x \frac{(20nm)}{100\ nm}$$
$$: 0.077424\ g/mL \sim 7.74\ g/100\ mL$$

According to the conversion above, the soy lecithin used was 7.74 g in 100 mL of re-distilled water.

In this study, the expected empirical size of nanoliposomes was 100 nm. However, due to the limitation in facility (computer speed and power), the simulation of

nanoliposomes formation with particle size of 100 nm was difficult to conduct in the *in silico* modeling. Hence, we converted the particle size into 20 nm which is equivalent to 0.077424 g/mL (7.74 g/100 mL) of soy lecithin where the simulation could be performed.

Determination of the particle size

The determination and distribution process in the system were conducted using particle size analyzer instrument, Horiba SZ-100, based on the scattering dynamic light principle with 25.0 °C temperature and 90° angle. 0.50 µL of the sample was transferred into a 25 mL volumetric flask, and then re-distilled water was added up to the calibration sign. A volume of 2.00 mL of aliquot was transferred into cuvet for the measurement of 100,000 particles.

Determination of a lamellar particle

The lamellar particle was observed using Transmission Electron Microscopy (TEM) JEM-1400 (Faculty of Natural Sciences, Gadjah Mada University, Indonesia). The determination of the lamellar particle was carried out on lipid nanoparticle with and without the presence of 4-*n*-butylresorcinol. A volume of 0.5 mL of the formula was added into 1 mL of re-distilled water, and then dropped into an object plate. The electromagnetic transmission light was subjected to the plate, and then the particle morphology was observed at a suitable magnitude. Morphological results of the sample were displayed on the camera screen with no staining process. The results were then visualized as the lamellar particle shape.

Results and discussion

The GC-MS of soy lecithin

GC-MS is used as this technique is suitable for lipid identification, in which the lipids are usually presented in an ester form (Naviglio et al., 2017). Ester is usually volatile; therefore, GC-MS is one of the suitable techniques to identify lipid both for its qualitative as well as quantitative prediction (Chiu & Kuo, 2020). Furthermore, GC-MS is a fast and cheap method, providing the compounds library which could easily predict the identified peak in GC chromatogram which corresponds to the mass spectrum when it is available in the database. The % similarity in the MS results enhances the power of this instrument to be utilized in determining the lipid. The ion source is electron impact 70 MeV resulting in fragmentation of the parent molecule into its most stable peak (base peak) accordingly. However, this technique has a disadvantage as the thermal stability of the compounds becomes the major issue (Koo et al., 2013). LC-MS could be the alternative method to reduce this thermal instability. Unfortunately, we could not perform this method at the moment due to our limitation. The soy lecithin contents were analyzed using GC-MS method. The retention time, percentage of peak area, and the base peaks as well as their interpretation are presented in Table 2.

In general, it was found that there were two primary compounds in soy lecithin, namely fatty acid and sterol (Table 3). The detected fatty acids were recognized as palmitic acid, oleic acid, and linoleic acid; whereas the sterol contents were recognized as clionasterol, 5-ergosterol, and stigmasterol.

Table 3 shows that only several lipids were detected and calculated by the GC-MS method due to their thermal instability during the analytical process. Therefore, the percentage of total area calculation was still below 100%. It can be seen that palmitate content was set at 54.32% since palmitate was found as a major compound in soy lecithin. Finally, the number of molecules for each lipid can be determined by multiplying the percentage and the total lipid, which can be seen in Table 4.

The potential energy calculation

The potential energy in the modeling of 2400, 2800, and 3200 phospholipid molecules were calculated. It can be noted that by increasing 4-*n*-butylresorcinol, the potential energy decreased (Table 5). The temperature was set to 50 °C during the simulation due to the protocol published in the previous study by Siwko et al. (2009). Figure 1 depicted the graphical plot of potential energy-time dependent which occurred during the simulation of 2400, 2800, and 3200 lipid molecules. The energy calculation involved in this study during the simulation processes were kinetic and potential energies.

The potential energy involved in the liposome formation describes that without 4-*n*-butylresorcinol (blue lines) (Figure 1), it tends to have higher potential energy than with 4-*n*-butylresorcinol (green lines). This indicates that a system having 4-*n*-butylresorcinol is more stable than the one without this active ingredient. The results are in line with the study performed by Siwko et al., in which the presence of resorcinol increased the liposome structural stability by joining the bilayer membrane while inducing a proper arrangement of the phospholipid acyl chain leading to a lipid head group hydration.

The potential energies employed during the liposome formation are electrostatic and vdW energies, which are visualized in Figure 2. Figure 2a indicates that the electrostatic energy declines along with the increasing number of the phospholipid molecules as well as the 4-*n*-butylresorcinol, and so does the vdW energy in Figure 2b. The total energy system in Figure 2d is the cumulative energy of kinetics (Figure 2c) and the potential energy of electrostatic (Figure 2a). From these graphs, the electrostatic and vdW are two of the most potential energies involved during the nanoliposome modeling. Although the electrostatic seems to contribute the most stable energy with the system having the largest molecule number of phospholipids, the presence of 4-*n*-butylresorcinol is predicted to increase the system stability by inducing the phospholipid acyl chain to stabilize the forming bilayer membrane. The vdW also contributes into the system stability as this energy profile (Figure 2b) is identical with the electrostatic energy (Figure 2a). In conjunction,

Table 2. GC-MS analysis results of soy lecithin.

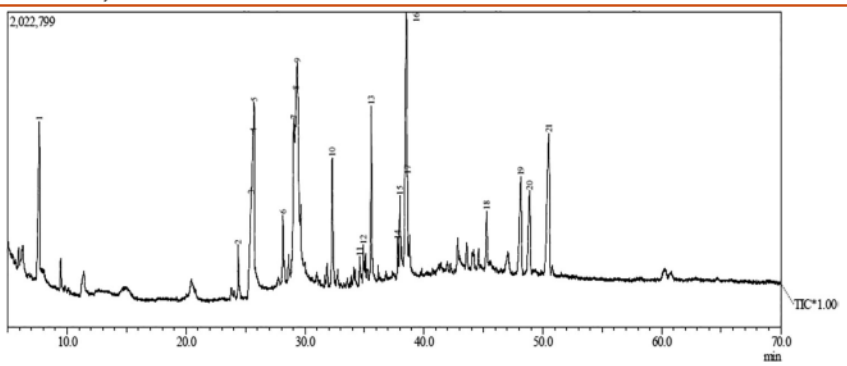

No	Peak #	Retention Time (minute)	Area (%)	Base peak (MW)	Interpreted as (MW)
1	2	24.38	1.49	74.05	Methyl palmitate (270)
2	5	25.73	5.42	43.10	Palmitic acid (256)
3	6	28.15	1.50	55.05	Methyl oleate (296)
4	9	29.35	11.17	55.10	Linoleic acid (280)
5	13	35.58	5.25	43.05	Glycerol 1-palmitate (330)
6	16	38.52	14.09	55.10	2-hydroxy-1-(hydroxymethyl)ethyl ester linolein (354)
7	18	45.28	1.89	43.10	Cholesteryl myristate
8	19	48.13	4.85	43.05	5-ergostenol (400)
9	20	48.90	3.98	55.10	Stigmasterol (412)
10	21	50.49	10.09	43.05	Clionasterol (414)

Note: only lipids and positive compound are shown.

Table 3. Soy lecithin primary component profiles.

Component	Peak #	% Area	Total % Area
Fatty acid			
Palmitate	2, 5, 13	1.49 + 5.42 + 5.25	12.16
Oleate	6	1.50	1.50
Linoleate	9, 16	11.17 + 14.09	25.26
		Total fatty acids	38.92
Sterol			
5-ergostenol	19	4.85	4.85
Stigmasterol	20	3.98	3.98
Clionasterol	21	10.09	10.09
		Total sterol	18.92

Table 4. Number of lipid molecules for each system in molecular modeling simulation.

System #	Number of lipids	DPPC	POPC	PIPC	Cholesterol
1	2400	1304	36	606	454
2	2800	1521	42	707	530
3	3200	1738	48	808	606

Note. DPPC = dipalmitoyl-phosphatidylcholine; POPC = palmitoyloleyl-phosphatidylcholine; PIPC = palmitoyllinoleyl-phosphatidylcholine.

the total energy (Figure 2d) is in proportion with the potential energy as depicted in Figure 2a and b, whereas the kinetic energy does not have the same trend. This different trend could be due to the kinetic energy being a fraction from the total energy system, so this could be neglected. In other words, the selected system is considered from the most stable energy profile, in which potential system employing electrostatic and vdW are the two best ones.

The radius of gyration of in silico modeling simulation

The radius of gyration can be described as a unit for the radius average from the molecule to the centre of mass to determine the liposome diameter. The radius of gyration allows to measure the nanoliposome formation during the simulation of 2400, 2800, and 3200 lipid molecules with and without the presence of *4-n*-butylresorcinol (Figure 3). The nanoliposomes morphological results of the simulation of 2400, 2800, and 3200 lipid molecules and their snapshots of nanoliposomes formation results during simulation can be seen in Figures 4 and 5, respectively. The liposome radii being formed during the simulation are shown in Figure 3a–c with a duplicate simulation. The results indicate that the liposome radii increases along with the increasing number of both phospholipid and *4-n*-butylresorcinol molecules.

The increasing liposome radii results in the increasing of the liposome size as its morphology is depicted in Figure 4. The shape of simulation having 2400 phospholipid molecules with *4-n*-butylresorcinol in the first replication is more likely less spherical than the second one (Figure 4a). The similar results occur in the system where 2800 phospholipid molecules with *4-n*-butylresorcinol show less imperfect spherical shape. Interestingly, the system with 3200 phospholipid molecules with *4-n*-butylresorcinol shows the most spherical shape among others, indicating its efficient atomic interactions between phospholipid and *4-n*-butylresorcinol. The inefficient atomic interactions could form the double connection between *4-n*-butylresorcinol and its corresponding phospholipid and other phospholipid leading to the final imperfect spherical structure. From this simulation, the system with 3200 phospholipid molecules is the most stable and reliable system predicted to produce liposome structure that will be used in the empirical study.

Table 5. The comparison between the time, the potential energy, and the shape of liposome being formed during the simulation with the number of lipids and 4-n-butylresorcinol treatment variation.

Number of lipids	*n*-butyl resorcinol	T enclosed (ns)	E1 (x10^6 kJ/mol)	E2 (x10^6 kJ/mol)	E3 (x10^6 kJ/mol)	Shape
2400	No	90	−2.947	−2.962	−2.963	Rod
		19	−2.942	−2.948	−2.952	Spherical
	Yes	56	−2.954	−2.968	−2.969	Elliptical
		31	−2.947	−2.953	−2.957	Spherical
2800	No	40	−2.941	−2.949	−2.951	Spherical with torus-shaped cavity
		20	−2.948	−2.956	−2.959	Spherical
	Yes	68	−2.947	−2.957	−2.959	Elliptical with U-shaped cavity
		18	−2.950	−2.955	−2.958	Spherical
3200	No	12	−2.937	−2.939	−2.945	Spherical
		24	−2.939	−2.941	−2.945	Spherical with crescent-shaped cavity
	Yes	32	−2.945	−2.953	−2.955	Spherical with torus-shaped cavity
		14	−2.950	−2.954	−2.958	Spherical

T = The time until liposome is fully enclosed.
E1 = The energy at 10 ns.
E2 = The energy when liposome is fully enclosed.
E3 = The energy at 240 ns.

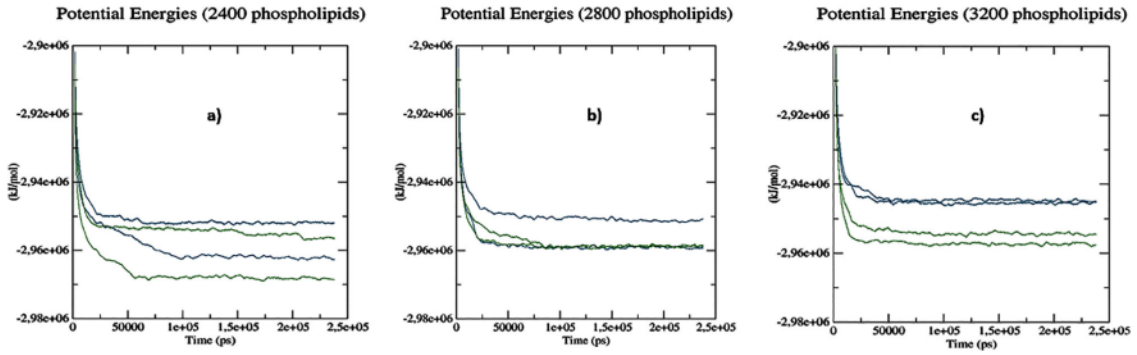

Figure 1. The graph plotting potential energy-time which occurred during the simulation of a) 2400, b) 2800, and c) 3200 lipid molecules. Note: Simulation with and without 4-*n*-butylresorcinol are shown by two green lines and two blue lines, respectively, as each treatment was performed in duplicate.

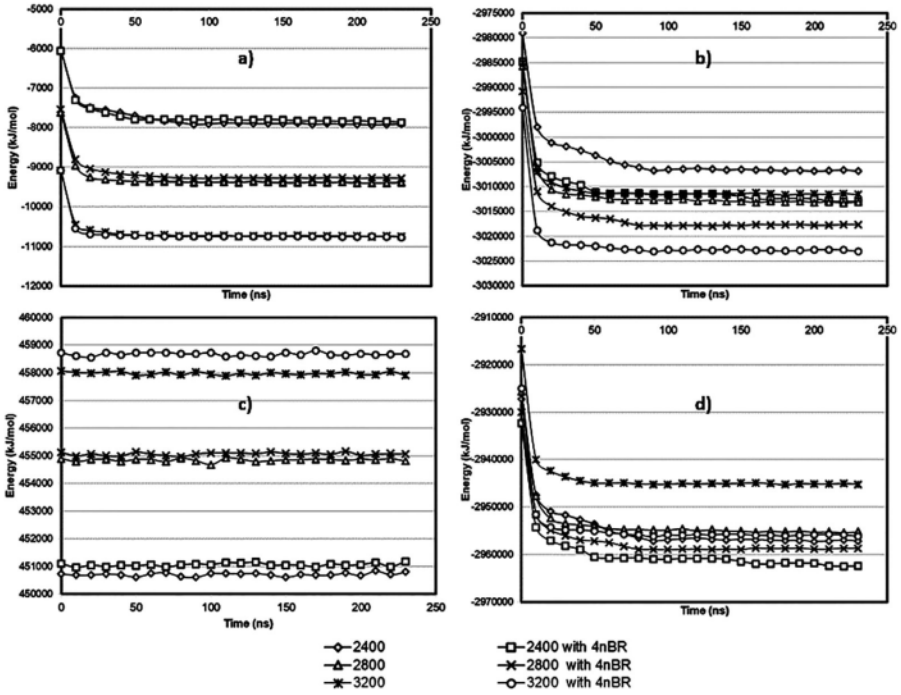

Figure 2. The graph plotting potential energy-time which occurred during the simulation of a) electrostatic, b) vdW, c) kinetic, and d) total energy.

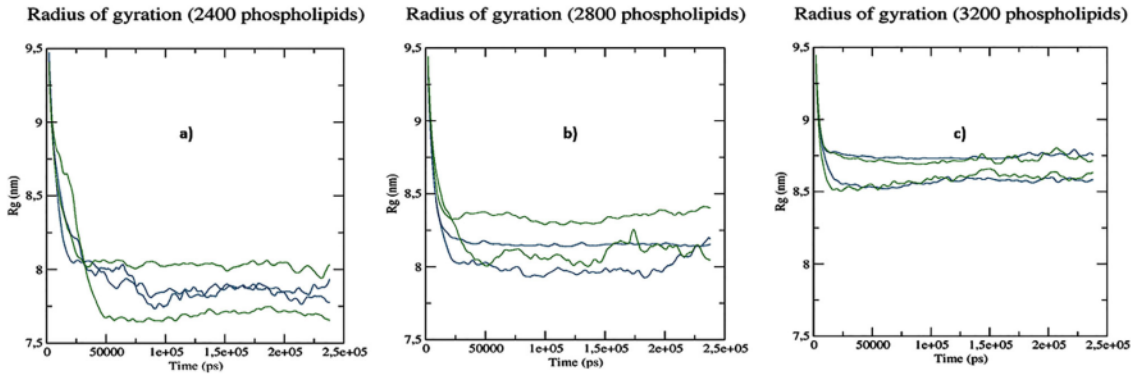

Figure 3. The gyration radius of the nanoliposomes being formed during the simulation of a) 2400, b) 2800, and c) 3200 of lipid molecules with (green) and without (blue) the presence of *4-n*-butylresorcinol.

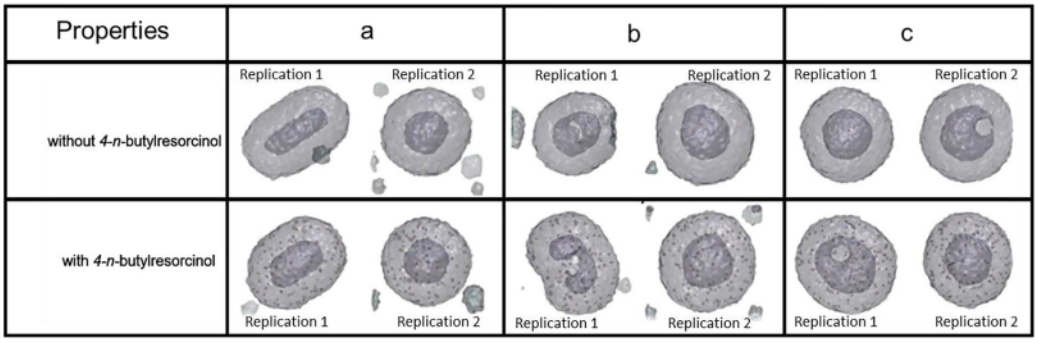

Figure 4. Nanoliposomes morphological results of the simulation of a) 2400, b) 2800, and c) 3200 lipid molecules with two replications for each lipid molecule number.

The size of nanoliposome with the presence of 4-n-Butylresorcinol

The size of nanoliposome resulted from both molecular dynamics simulations and empirical observations were compared and presented in Table 6. In this presentation, the empirical liposome was prepared from the selected system only (3200 phospholipid molecules with *4-n*-butylresorcinol) because this system showed the most stable energy profile as well as its morphology. The distribution curve of the nanoliposome size can be seen in Figure 6, demonstrating the population of liposome particle size with three times replications which shows the consecutive mode values i.e. 87.60, 87.50, and 87.60 nm with the standard deviation value of 0.06. The mode value is chosen to represent the liposome size distribution because it represents the largest frequency of the liposome size, which is generated in the empirical study. The distribution curves exhibit a similar pattern so that it indicates a good repeatability in the particle size of the liposome.

The morphology of 3200 phospholipid molecules

The morphological observation of 3200 phospholipid molecules from the simulation model was compared to the empirical observation without the presence of 4-*n*-butylresorcinol, which can be seen in Figure 7. In addition, the interaction between drug and the membrane model is depicted in Figure 8.

The GC-MS method was utilized to determine the chemical composition of the soy lecithin as listed in Table 2. The fatty acids of the phospholipid and sterol were used as the platform in the nanoliposomes modeling. The identified compositions of fatty acid from the GC-MS were palmitic acid, oleic acid, and linoleic acid. Theoretically, it is appropriate with the composition of soy lecithin (Perkins, 1995; Van Hoogevest et al., 2013). The sterol being composed in the soy lecithin was 5-ergosterol, stigmasterol, and clionasterol (Table 3). The percentage of fatty acid and sterol as calculated in Table 3 was used as the basic calculation to decide the composition of the nanoliposomes modeling.

The nanoliposomes modeling with and without the presence of 4-*n*-butylresorcinol used three variations of the lipid molecule number, i.e. 2400, 2800, and 3200 molecules. This observation was aimed to predict the possibility of the nanoliposomes formation with and without the presence of 4-*n*-butylresorcinol by modeling on a few lipid molecules used. The decision of selecting the number of lipid molecules was applied and referred to the study conducted by Koshiyama and Wada (2016). The results indicated a formation of nanoliposomes from modeling using 2400, 2800 and 3200 molecules inside a 22 nm^3 size box (Figure 2).

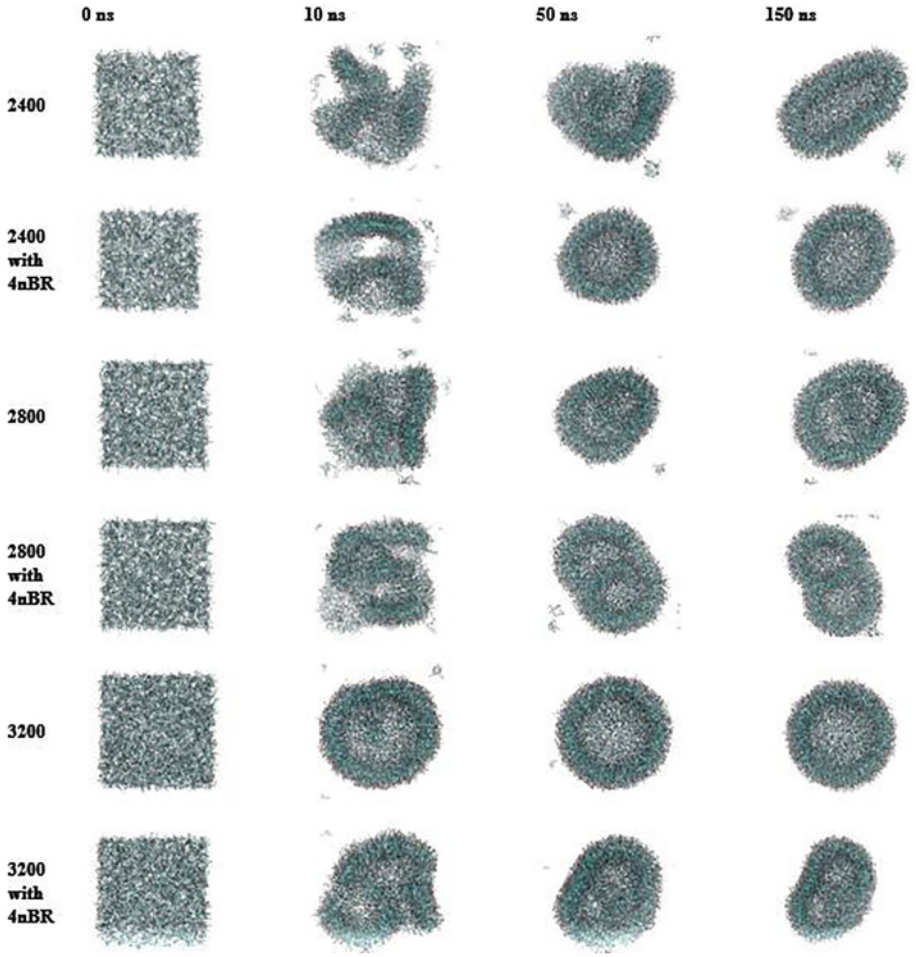

Figure 5. Snapshots of nanoliposomes formation results during the simulation.

Table 6. Results of nanoliposome size based on simulation and empirical observation for 4-n-butylresorcinol.

Nanoliposome sizes based on the *in silico* simulations (3200 molecules)		Nanoliposome sizes based on the empirical observation		
Replication	Nanoliposome sizes (nm)	Replication	Calculation mode (nm)	Polydispersity Index
1	86.60	1	87.60	0.28
2	87.43	2	87.50	0.18
		3	87.60	0.24
Mean (±SD)	87.01 (± 0.59)	Mean (±SD)	87.57 (± 0.06)	

According to the graphical energy presented in Figures 1 and 2, the potential energies were stronger for a lower lipid number. This trend appears in the lower number of lipids and the higher number of water, which contributes to stronger electrostatic and vdW interactions. In terms of the velocity and stability, both the energy graph as well as the radius of gyration graph show that at a higher number of lipids, the liposomes are formed faster and quickly stabilized. It is also important to note that the slower liposome formation tends to give the phospholipid bilayer a chance to form a multiple connection, leading to an imperfect sphere or a bilayer bridge in the middle of the liposome (see Figure 4b). Therefore, the 3200 lipids molecule was subjected to the empirical nanoliposomes formulation with and without the presence of 4-*n*-butylresorcinol. The formation of nanoliposomes in the molecular modeling involves kinetic and potential energies in the form of electrostatic and vdW interactions. According to the energy calculation results in the modeling simulation at 50 °C, the nanoliposome system was stable at about 100 ns (Figures 1 and 2). Nanoliposome structures were generated in the modeling simulation with electrostatic energy. It may result from the interaction between electronegative atoms in the phosphate group of the phospholipid with the hydrogen atom from the water molecules around the system. Furthermore, an electrostatic interaction between polar groups of phospholipid during simulation also occurs. The lower vdW energy indicates a similar graphical profile with lower electrostatic and total

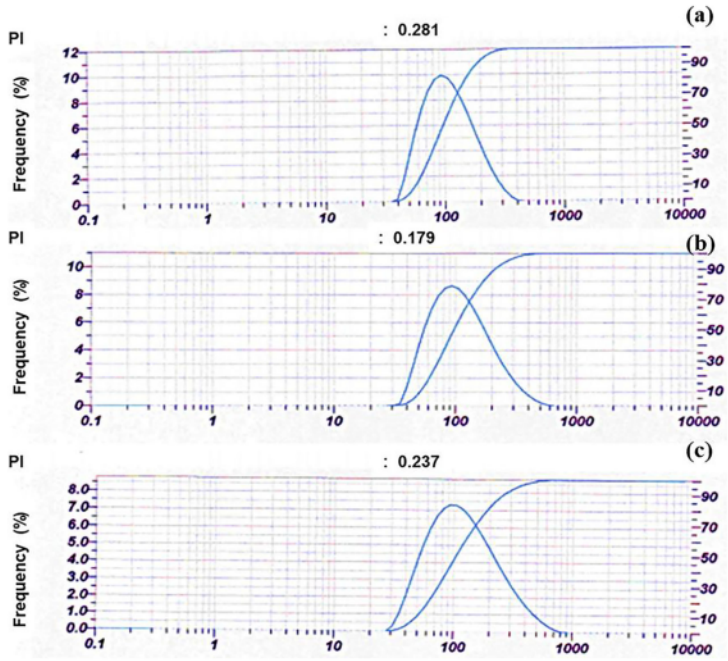

Figure 6. The nanoliposome size distribution curves in triplicate measurements exhibit a similar population with their consecutive mode values i.e. 87.60 (a), 87.50 (b), and 87.60 nm (c) having polydispersity index (PI) of 0.281, 0.179, and 0.237, respectively.

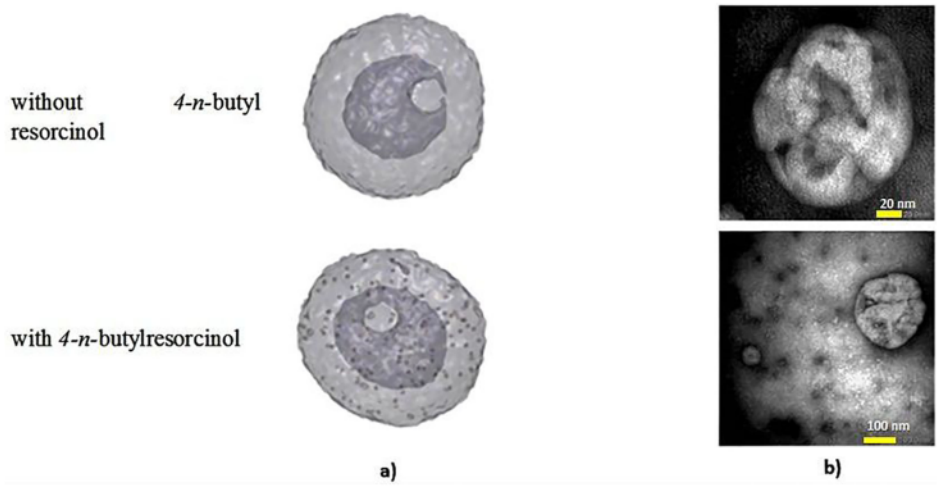

Figure 7. The nanoliposome morphology being formed from a) the modeling and b) the empirical observation on 3200 lipid molecules.

energy in the system. The interaction between non-polar group during the simulation resulted in vdW energy. With the longer simulation time, the electrostatic, vdW, and the total energy were decreased due to the system stabilization in order to achieve the nanoliposomes structure (Figure 5) for simulation, with and without *4-n*-butylresorcinol in three different molecules number (2400, 2800, and 3200). The system stabilization has been achieved when the unilamellar nanoliposomes was formed in 100 ns. Moreover, the electrostatic, vdW, and total energies decreased in both systems with and without *4-n*-butylresorcinol during the simulation. The vdW energy depicted interactions between non-polar groups of phospholipid molecules and non-polar group of *4-n*-butylresorcinol. Chemical properties of the non-polar model compound might affect the vdW interaction at the initial and at the end of the simulation. The interaction between 4-*n*-butylresorcinol-lipid and lipid-membrane during the simulation process resulted in similar characteristic results with the previous study (Siwko et al., 2009), where the hydroxyl (-OH) group of *4-n*-butylresorcinol interacted with the hydrophilic group of the phospholipid compound (Figure 7). The presence of *4-n*-butylresorcinol increased the vdW interaction between non-polar groups, whereas the electrostatic interaction in phosphate group with hydrogen

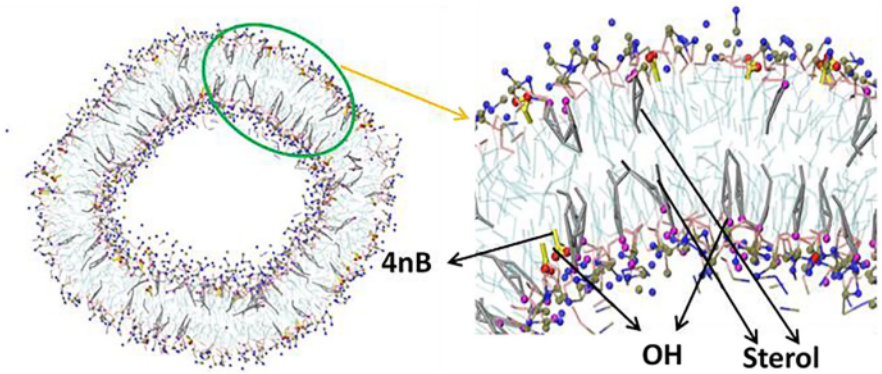

Figure 8. The interaction of the model compound in the lipid membrane.

atom from water was decreased since there was several hydrogen bonding between the two phospholipid molecules. The morphological results of the simulation (Figure 5) indicated that nanoliposomes were formed into unilamellar structure. The simulation with 3200 phospholipid molecules resulted in a similar form of nanoliposomes compared to the empirical observation results (Figure 6).

The conversion of the phospholipid from the simulation was done using a concentration of 3200 molecules by 0.38712 g/mL with the conversion factor of 0.2. This factor was a ratio between the box size used in the simulation (20 nm) and the actual box that should be used in the empirical observation, i.e. 100 nm. The parameter being observed in the nanoliposomes product was the size and the morphology of the nanoliposomes being formed. The nanoliposomes size in the molecular modeling of 3200 lipid molecules was 87.01 nm (± 0.59), whereas the size from the empirical study was 87.57 (± 0.06). These results indicated that there was no significant difference for the size and the morphology of nanoliposomes formed with and without the presence of 4-*n*-butylresorcinol. However, this study has some limitations in that no physicochemical parameter evaluation and empirical studies for 2400 and 2800 phospholipid molecules are conducted, which prompts us to do these experiments in our future study.

Conclusions

Molecular dynamics simulation was proven to be the tool that strongly predicts the dynamics behavior of 4-*n*-butylresorcinol upon nanoliposome formulation. The program was able to predict the number of phospholipid molecule during the formulation which resulted in agreement between *in silico* and empirical study. It was found that phospholipid molecules with the number of 3200 were selected in the formulation process of nanoliposome containing 4-*n*-butylresorcinol. The modeling and empirical studies resulted in the molecules size of 87.01 (± 0.59) and 87.57 (± 0.06) nm, respectively. These significant results indicated the connection between the *in silico* modeling and the empirical observation in formulating nanoliposome.

Disclosure statement

No potential conflict of interest was reported by the authors.

Funding

We gratefully acknowledge The Ministry of Research and Technology of Higher Education for funding under the Research Grant with contract letter no: 029/Penel./LPPM-USD/IV/2019.

References

Akbarzadeh, A., Rezaei-Sadabady, R., Davaran, S., Joo, S. W., Zarghami, N., Hanifehpour, Y., Samiei, M., Kouhi, M., & Nejati-Koshki, K. (2013). Liposome: Classification, preparation, and applications. *Nanoscale Research Letters*, *8*(1), 1–9. https://doi.org/10.1186/1556-276X-8-102

Boisseau, P., & Loubaton, B. (2011). Nanomedicine, nanotechnology in medicine. *Comptes Rendus Physique*, *12*(7), 620–636. https://doi.org/10.1016/j.crhy.2011.06.001

Cem, A., Barenholz, Y., Tropsha, A., & Goldblum, A. (2014). Computer-aided design of liposomal drugs: In silico prediction and experimental validation of drug candidates for liposomal remote loading. *Journal of Controlled Release : official Journal of the Controlled Release Society*, *173*, 125–131. https://doi.org/10.1016/j.jconrel.2013.10.029

Cem, A., Marcus, D., Tropsha, A., Barenholz, Y., & Goldblum, A. (2017). New drug candidates for liposomal delivery identified by computer modeling of liposomes' remote loading and leakage. *Journal of Controlled Release: Official Journal of the Controlled Release Society*, *252*, 18–27. https://doi.org/10.1016/j.jconrel.2017.02.015

Chiu, H. H., & Kuo, C. H. (2020). Gas chromatography-mass spectrometry-based analytical strategies for fatty acid analysis in biological samples. *Journal of Food and Drug Analysis*, *28*(1), 60–73. https://doi.org/10.1016/j.jfda.2019.10.003

Coradini, K., Lima, F. O., Oliveira, C. M., Chaves, P. S., Athayde, M. L., Carvalho, L. M., & Beck, R. (2014). Co-encapsulation of resveratrol and curcumin in lipid-core nanocapsules improves their in vitro antioxidant effects. *European Journal of Pharmaceutics and Biopharmaceutics*, *88*(1), 178–185. https://doi.org/10.1016/j.ejpb.2014.04.009

De Leeuw, J., De Vijlder, H. C., Bjerring, P., & Neumann, H. A. M. (2009). Liposomes in dermatology today. *Journal of the European Academy of Dermatology and Venereology: JEADV*, *23*(5), 505–516. https://doi.org/10.1111/j.1468-3083.2009.03100.x

Dogra, P., Butner, J. D., Chuang, Y. L., Caserta, S., Goel, S., Brinker, C. J., Cristini, V., & Wang, Z. (2019). Mathematical modeling in cancer nanomedicine: A review. *Biomedical Microdevices*, *21*(2), 1–23. https://doi.org/10.1007/s10544-019-0380-2

Dwiastuti, R., Noegrohati, S., Istyastono, E. P. Marchaban, (2016). Formulation and physical properties observations of soy lecithin liposome containing 4-n-butylresorcinol. In *AIP Conference Proceedings* (Vol. 1755, No. 1, p. 160005). AIP Publishing LLC.

Dwiastuti, R., Radifar, M., Marchaban, M., Noegrohati, S., & Istyastono, E. P. (2018). Molecular dynamics simulations and empirical observations on soy lecithin liposome preparation. *Indonesian Journal of Chemistry*, *16*(2), 222–228. https://doi.org/10.22146/ijc.21167

Eloy, J. O., de Souza, M. C., Petrilli, R., Barcellos, J. P. A., Lee, R. J., & Marchetti, J. M. (2014). Liposomes as carriers of hydrophilic small molecule drugs: Strategies to enhance encapsulation and delivery. *Colloids and Surfaces. B, Biointerfaces*, *123*, 345–363. https://doi.org/10.1016/j.colsurfb.2014.09.029

Hashemzadeh, H., Javadi, H., & Darvishi, M. H. (2020). Study of Structural stability and formation mechanisms in DSPC and DPSM liposomes: A coarse-grained molecular dynamics simulation. *Scientific Reports*, *10*(1), 1837. https://doi.org/10.1038/s41598-020-58730-z

Hudiyanti, D., Radifar, M., Raharjo, T. J., Narsito, N., & Noegrohati, S. (2014). A coarse-grained molecular dynamics simulation using NAMD package to reveal aggregation profile of phospholipids self-assembly in water. *Journal of Chemistry*, *2014*, 1–6. https://doi.org/10.1155/2014/273084

Huh, S. Y., Shin, J. W., Na, J. I., Huh, C. H., Youn, S. W., & Park, K. C. (2010). Efficacy and safety of liposome-encapsulated 4-n-butylresorcinol 0.1% cream for the treatment of melasma: a randomized controlled split-face trial . *The Journal of Dermatology*, *37*(4), 311–315. https://doi.org/10.1111/j.1346-8138.2010.00787.x

Jämbeck, J. P. M., Eriksson, E. S. E., Laaksonen, A., Lyubartsev, A. P., & Eriksson, L. A. (2014). Molecular dynamics studies of liposomes as carriers for photosensitizing drugs: development, validation, and simulations with a coarse-grained model. *Journal of Chemical Theory and Computation*, *10*(1), 5–13. https://doi.org/10.1021/ct400466m

Khemis, A., Kaiafa, A., Queille-Roussel, C., Duteil, L., & Ortonne, J. P. (2007). Evaluation of efficacy and safety of rucinol serum in patients with melasma: A randomized controlled trial. *British Journal of Dermatology*, *156*(5), 997–1004. https://doi.org/10.1111/j.1365-2133.2007.07814.x

Kolbe, L., Mann, T., Gerwat, W., Batzer, J., Ahlheit, S., Schemer, C., Wenck, H., & Stäb, F. (2013). 4-n-butylresorcinol, a highly effective tyrosinase inhibitor for the topical treatment of hyperpigmentation. *Journal of the European Academy of Dermatology and Venereology*, *27*, 19–23. https://doi.org/10.1111/jdv.12051

Koo, I., Kim, S., & Zhang, X. (2013). Comparative analysis of mass spectral matching-based compound identification in gas chromatography-mass spectrometry. *Journal of Chromatography. A*, *1298*, 132–138. https://doi.org/10.1016/j.chroma.2013.05.021

Koshiyama, K., & Wada, S. (2016). Collapse of a lipid-coated nanobubble and subsequent liposome formation. *Scientific Reports*, *6*(1), 1–8. https://doi.org/10.1038/srep28164

Laouini, A., Jaafar-Maalej, C., Limayem-Blouza, I., Sfar, S., Charcosset, C., & Fessi, H. (2012). Preparation, characterization and applications of liposomes: State of the art. *Journal of Colloid Science and Biotechnology*, *1*(2), 147–168. https://doi.org/10.1166/jcsb.2012.1020

Li, Y., & Hou, T. (2010). Computational simulation of drug delivery at molecular level. *Current Medicinal Chemistry*, *17*(36), 4482–4491. https://doi.org/10.2174/092986710794182935

Love, A. R., Kerschner, J. L., Barratt, M. J., & Zhou, Y. (2005). *U.S. Patent* No. 6863897. U.S. Patent and Trademark Office.

Maghraby, G. M. E., Williams, A. C., & Barry, B. W. (2010). Skin delivery of 5-fluorouracil from ultradeformable and standard liposomes in-vitro. *Journal of Pharmacy and Pharmacology*, *53*(8), 1069–1077. https://doi.org/10.1211/0022357011776450

Maghraby, G. M. E., Williams, A. C., & Barry, B. W. (2010). Skin delivery of oestradiol from deformable and traditiona liposomes: Mechanistic studies. *Journal of Pharmacy and Pharmacology*, *51*(10), 1123–1134. https://doi.org/10.1211/0022357991776813

Martien, R., Adhyatmika, A., Irianto, I. D., Farida, V., & Sari, D. P. (2012). Perkembangan teknologi nanopartikel sebagai sistem penghantaran obat. *Majalah Farmaseutik*, *8*(1), 133–144.

Mozafari, M. R., Reed, C. J., & Rostron, C. (2007). Prospects of anionic nanolipoplexes in nanotherapy: Transmission electron microscopy and light scattering studies. *Micron (Oxford, England: 1993)*, *38*(8), 787–795. https://doi.org/10.1016/j.micron.2007.06.007

Naviglio, D., Dellagreca, M., Ruffo, F., Andolfi, A., & Gallo, M. (2017). Rapid analysis procedures for triglycerides and fatty acids as pentyl and phenethyl esters for the detection of butter adulteration using chromatographic techniques. *Journal of Food Quality*, *2017*, 1–11. https://doi.org/10.1155/2017/9698107

Perkins, E. G. (1995). Composition of soybeans and soybean products. In *Practical handbook of soybean processing and utilization* (pp. 9–28). AOCS Press.

Puri, A., Loomis, K., Smith, B., Lee, J. H., Yavlovich, A., Heldman, E., & Blumenthal, R. (2009). Lipid-based nanoparticles as pharmaceutical drug carriers: From concepts to clinic. *Critical Reviews™ in Therapeutic Drug Carrier Systems*, *26*(6), 523–580.

Reverchon, E., & Adami, R. (2006). Nanomaterials and supercritical fluids. *The Journal of Supercritical Fluids*, *37*(1), 1–22. https://doi.org/10.1016/j.supflu.2005.08.003

Risselada, H. J., & Marrink, S. J. (2009). Curvature effects on lipid packing and dynamics in liposomes revealed by coarse grained molecular dynamics simulations. *Physical Chemistry Chemical Physics: PCCP*, *11*(12), 2056–2067. https://doi.org/10.1039/b818782g

Shen, K. C., Kakumanu, S., Beckett, C. D., & Laugharn, J. A. Jr (2015). Use of Adaptive Focused Acoustics™ ultrasound in controlling liposome formation. *Ultrasonics Sonochemistry*, *27*, 638–645. https://doi.org/10.1016/j.ultsonch.2015.04.027

Silva, R., Ferreira, H., Little, C., & Cavaco-Paulo, A. (2010). Effect of ultrasound parameters for unilamellar liposome preparation. *Ultrasonics Sonochemistry*, *17*(3), 628–632. https://doi.org/10.1016/j.ultsonch.2009.10.010

Singh, M., Manikandan, S., & Kumaraguru, A. K. (2011). Nanoparticles: A new technology with wide applications. *Research Journal of Nanoscience and Nanotechnology*, *1*(1), 1–11. https://doi.org/10.3923/rjnn.2011.1.11

Siwko, M. E., de Vries, A. H., Mark, A. E., Kozubek, A., & Marrink, S. J. (2009). Disturb or stabilize? A molecular dynamics study of the effects of resorcinolic lipids on phospholipid bilayers. *Biophysical Journal*, *96*(8), 3140–3153. https://doi.org/10.1016/j.bpj.2009.01.040

Trisilowati., & Mallet, D. G. (2012). *In silico* experimental modeling of cancer treatment. *ISRN Oncology*, *2012*, 1–8. https://doi.org/10.5402/2012/828701

Van Hoogevest, P., Prusseit, B., & Wajda, R. (2013). Phospholipids: Natural functional ingredients and actives for cosmetic products. *SOFW-Journal*, *8*(9), 14.

Wang, S., Zhang, J., Jiang, T., Zheng, L., Wang, Z., Zhang, J., & Yu, P. (2011). Protective effect of Coenzyme Q(10) against oxidative damage in human lens epithelial cells by novel ocular drug carriers. *International Journal of Pharmaceutics*, *403*(1-2), 219–229. https://doi.org/10.1016/j.ijpharm.2010.10.020

Zhao, L., Wei, Y. M., Zhong, X. D., Liang, Y., Zhang, X. M., Li, W., Li, B., Wang, Y., & Yu, Y. (2009). PK and tissue distribution of docetaxel in rabbits after iv administration of liposomal and injectable formulations. *Journal of Pharmaceutical and Biomedical Analysis*, *49*(4), 989–996. https://doi.org/10.1016/j.jpba.2009.01.016

In silico modeling and empirical study of 4-nButylresorcinol nanoliposome formulation

ORIGINALITY REPORT

11%	10%	8%	4%
SIMILARITY INDEX	INTERNET SOURCES	PUBLICATIONS	STUDENT PAPERS

PRIMARY SOURCES

1	protres.ru Internet Source	1%
2	www.degruyter.com Internet Source	1%
3	Submitted to Taibah University Student Paper	1%
4	repository.usd.ac.id Internet Source	1%
5	link.springer.com Internet Source	1%
6	Joakim P. M. Jämbeck, Emma S. E. Eriksson, Aatto Laaksonen, Alexander P. Lyubartsev, Leif A. Eriksson. "Molecular Dynamics Studies of Liposomes as Carriers for Photosensitizing Drugs: Development, Validation, and Simulations with a Coarse-Grained Model", Journal of Chemical Theory and Computation, 2013 Publication	1%

7	jurnal.ugm.ac.id Internet Source	1 %
8	Sun Young HUH. "Efficacy and safety of liposome-encapsulated 4-*n*-butylresorcinol 0.1% cream for the treatment of melasma: A randomized controlled split-face trial", The Journal of Dermatology, 04/2010 Publication	<1 %
9	digitalcommons.library.umaine.edu Internet Source	<1 %
10	core.ac.uk Internet Source	<1 %
11	www.sciencegate.app Internet Source	<1 %
12	research.snu.edu.in Internet Source	<1 %
13	Submitted to Universitas Sanata Dharma Student Paper	<1 %
14	Submitted to Virginia Commonwealth University Student Paper	<1 %
15	elea.unisa.it Internet Source	<1 %
16	e-journal.unair.ac.id Internet Source	<1 %

17	research-information.bris.ac.uk Internet Source	<1 %
18	studentsrepo.um.edu.my Internet Source	<1 %
19	Alhara Yuwanda, Silvia Surini, Yahdiana Harahap, Mahdi Jufri. "Study of valproic acid liposomes for delivery into the brain through an intranasal route", Heliyon, 2022 Publication	<1 %
20	Veronika Valková, Hana Ďúranová, Aude Falcimaigne-Cordin, Claire Rossi et al. "Impact of Freeze- and Spray-Drying Microencapsulation Techniques on β-Glucan Powder Biological Activity: A Comparative Study", Foods, 2022 Publication	<1 %
21	Xue-Feng Lu, Kaishun Bi, Xiaohui Chen. "Physiologically based pharmacokinetic model of docetaxel and interspecies scaling: comparison of simple injection with folate receptor-targeting amphiphilic copolymer-modified liposomes", Xenobiotica, 2016 Publication	<1 %
22	ugspace.ug.edu.gh Internet Source	<1 %
23	Percutaneous Penetration Enhancers Chemical Methods in Penetration	<1 %

Enhancement, 2016.
Publication

24	archive-ouverte.unige.ch Internet Source	<1 %
25	crossmark.crossref.org Internet Source	<1 %
26	dokumen.pub Internet Source	<1 %
27	eprints.nottingham.ac.uk Internet Source	<1 %
28	mdpi-res.com Internet Source	<1 %
29	publications.waset.org Internet Source	<1 %
30	repositorio.unican.es Internet Source	<1 %
31	Muhammad Khan, Jangsun Hwang, Kyungwoo Lee, Yonghyun Choi, Kyobum Kim, Hyung-Jun Koo, Jong Hong, Jonghoon Choi. "Oxygen-Carrying Micro/Nanobubbles: Composition, Synthesis Techniques and Potential Prospects in Photo-Triggered Theranostics", Molecules, 2018 Publication	<1 %
32	Viet Hoang Man, Phan Minh Truong, Mai Suan Li, Junmei Wang, Nguyen-Thi Van-Oanh,	<1 %

	Philippe Derreumaux, Phuong Hoang Nguyen. "Molecular Mechanism of the Cell Membrane Pore Formation Induced by Bubble Stable Cavitation", The Journal of Physical Chemistry B, 2018 Publication	
33	library.unisel.edu.my Internet Source	<1 %
34	repositorio.unifesp.br Internet Source	<1 %
35	www.frontiersin.org Internet Source	<1 %
36	www.mdpi.com Internet Source	<1 %
37	H. Chamati, R. Trobec, J.I. Pavlič. "Peculiarities in the Study of Preformed DSPC Lipid Vesicles by Coarse Grain Molecular Dynamics", Elsevier BV, 2016 Publication	<1 %

Exclude quotes	Off	Exclude matches	Off
Exclude bibliography	On		